Results in Optics 5 (2021) 100123

Contents lists available at ScienceDirect

Results in Optics

journal homepage: www.sciencedirect.com/journal/results-in-optics

Invited Article

Nanocoated fiber label-free biosensing for perfluorooctanoic acid detection by lossy mode resonance

Giulia Moro [a,b,c], Francesco Chiavaioli [d,*], Stefano Liberi [e], Pablo Zubiate [f], Ignacio Del Villar [f,g], Alessandro Angelini [a,h], Karolien De Wael [b,c], Francesco Baldini [d], Ligia Maria Moretto [a], Ambra Giannetti [d]

[a] Department of Molecular Sciences and Nanosystems, Ca' Foscari University of Venice, Via Torino 155, 30172 Mestre, Italy
[b] AXES Research Group, University of Antwerp, Groenenborgerlaan 171, 2020, Antwerp, Belgium
[c] NanoLab Center of Excellence, University of Antwerp, Groenenborgerlaan 171, 2020 Antwerp, Belgium
[d] Institute of Applied Physics "Nello Carrara", National Research Council of Italy (CNR), 50019 Sesto Fiorentino, Firenze, Italy
[e] Department of Biology, University of Padua, Via U. Bassi 58, 35131 Padova, Italy
[f] Electrical and Electronic Engineering Department, Public University of Navarra, 31006 Pamplona, Spain
[g] Institute of Smart Cities (ISC), Public University of Navarra, 31006 Pamplona, Spain
[h] European Centre for Living Technology (ECLT), Ca' Bottacin, Dorsoduro 3911, Calle Crosera, 30123 Venice, Italy

ARTICLE INFO

Keywords:
Nanocoated fiber sensor
Lossy mode resonance
Small target detection
Delipidated human serum albumin
Perfluorooctanoic acid
Label-free biosensing

ABSTRACT

The determination of per- and polyfluoroalkyl substances (PFAS) in environmental samples, such as drinking waters, requires the design of high performing and versatile sensing strategies. Label-free biosensing platforms based on specialty fiber optics are a valid option to face this challenge. Among them, lossy mode resonance (LMR) fiber optic biosensors are showing remarkable performance in terms of detection limit, selectivity, and reproducibility. The detection of small molecules, such as perfluorooctanoic acid (PFOA), can be achieved with the help of well-designed biological recognition layers. In this study, the biosensing potentialities of a label-free LMR-assisted optical platform based on nanocoated fibers are investigated. Delipidated human serum albumin (hSA) was used as biological recognition layer for PFOA in aqueous solution. Different fiber functionalization protocols based on the covalent immobilization of hSA were tested. The conformational changes related to the formation of hSA/PFOA complex were followed via optical monitoring of LMR spectral shift, showing a trend that can be modeled with Langmuir adsorption isotherm. These results confirmed the potentiality of LMR-based fiber biosensors for the detection of small molecules, such as PFOA, in synthetic samples.

1. Introduction

Optical sensors are largely applied in the analysis of drugs, pesticide residues, pathogens, heavy metals, toxic substances, as well as other environmental pollutants (Khansili et al., 2018). Among them, fiber optic (FO)-based sensors for water pollutants monitoring can provide highly sensitive, selective and reproducible responses (Zhang et al., 2020; Jiao et al., 2020). The easiness of combining FOs with other sensing elements, (i.e. metal nanoparticles, quantum dots or inorganic/polymeric nanocoatings) made possible the design of a wide variety of sensing strategies that allow modifying the optical features and, as a consequence, the performance of the final device (Nazri et al., 2021; Shukla et al., 2019; Wang and Wolfbeis, 2020; Li et al., 2021; Esposito et al., 2021).

FOs can be successfully integrated within microfluidic systems for the detection of biomolecules, from nucleic acids to cells, and other chemicals (Zhao et al., 2020). The design of these platforms together with other miniaturized systems is particularly suitable for water monitoring applications where the compatibility with on-flow system is often required (Meyer et al., 2019; Yaroshenko et al., 2020). The recent progresses in FO manufacturing and functionalization, the development of "Lab-on-Fiber" tools and their wide application in food safety, health and environmental monitoring suggest the interest for these technologies (Ricciardi et al., 2015; Pissadakis, 2019). Different strategies can be adopted to allow the interaction of light traveling inside the fiber with the surrounding environment, with the simplest one constituted by the

* Corresponding author.
E-mail address: f.chiavaioli@ifac.cnr.it (F. Chiavaioli).

https://doi.org/10.1016/j.rio.2021.100123
Received 21 May 2021; Accepted 26 July 2021
Available online 29 July 2021

etching of the fiber cladding up to its entire removal, which leads to the extension of the evanescent wave of fiber mode (electromagnetic field) outside the fiber (Cardona-Maya et al., 2018; Śmietana et al., 2016). The use of suitable micro/nanocoatings can enhance this effect thanks to the fact that light can be guided within the applied coatings and leaks more out the fiber with a stronger extent (Li et al., 2021; Chiavaioli, 2020). Depending on the implemented sensing concept, on the deposited coating, and on the FO features, surface plasmon polaritons, Bloch or lossy/leaky mode waves can be generated to exploit the excitation of resonance-based phenomena (Chiavaioli, 2020), such as surface plasmon resonance (SPR) (Homola, 2003) or other mode resonances. All these optical resonances can be used to measure the changes in the fiber-surrounding refractive index (RI) on the basis of induced shift of the resonance wavelength (Chiavaioli et al., 2017; Chiavaioli and Janner, 2021).

Among the resonance-based phenomena, lossy mode resonance (LMR) has several advantages over the well-established SPR, such as easy tunability of the LMR wavelength in the optical spectrum as a function of the coating thickness, cheaper material used as coating (metal-oxides or polymers with respect to noble metals), possibility of exciting both TE and TM polarization states of light and capability of multiple LMR generation above all. To have a highly sensitive response in LMR, the waveguide modes need to be coupled with a particular lossy mode of the semi-conductor nanocoating and an optimal film thickness value can allow obtaining a maximum attenuation in the transmission spectrum. Therefore, the control and characterization of the nanocoating thickness play a key-role in LMR-based sensors, as described by Del Villar et al. (Del Villar et al., 2012). In this context, the nanomaterial that showed the highest RI sensitivity is tin dioxide (SnO_{2-x}) in comparison with other LMR-exciting nanomaterials (Kosiel et al., 2018; Zubiate et al., 2019). As recently highlighted (Chiavaioli et al., 2018; Chiavaioli and Janner, 2021), the FO geometry is doubtless another feature to take into account in the design of high-performance sensing platforms. Till now, the configuration that experimentally provides the best performance makes use of D-shaped or side-polished single-mode FO. A scheme of a D-shaped FO nanocoated with a layer of SnO_{2-x} and an additional polymeric nano-film for surface functionalization is reported in Fig. 1A, as example of the type of fibers used in the present work. Despite the versatility of these optical platforms in label-free biosensing, their capability to detect small molecules is extremely limited due to the non-chromogenic/fluorescent nature of the analyte (in this case a labeled-based approach must be used as single molecule array methodology (Schubert et al., 2015) or its low molecular weight. So far, this challenge was faced by implementing the instrumentation and methodologies in use, including immobilization steps or receptors, as overviewed by Peltomaa et al. (Peltomaa et al., 2018).

In the field of the environmental pollutants, per- and polyfluoroalkyl substances (PFAS) represent a class of widely used, man-made forever chemicals which bioaccumulate in humans and in the environment with harmful effects to our health and ecosystems (Fiedler et al., 2020; Nakayama et al., 2019). During the last decade, these findings ignited a lively debate in the scientific and regulatory community leading to the urgent request of strict regulatory actions against PFAS pollution (Wang et al., 2018; Kwiatkowski et al., 2020), the discussion about PFOA reported by Vierke et al. is a representative example (Vierke et al., 2012). In this frame, particularly relevant are the PFAS maximum concentration levels in drinking water and groundwater suggested by environmental agencies, such as EPA (Environmental Protection Agency, U.S. A.) and EEA (European Environmental Agency, E.U.) (Abunada et al., 2020; Dean et al., 2020). These values are mostly lower than 100 ng L^{-1}, while environmental reports show that PFAS levels in water matrices exceed even the 1000 ng L^{-1} (Goodrow et al., 2020; Bertanza et al., 2020).

The large number of fluorinated chemicals, the variety of contaminated matrices (i.e. ground waters, soils, plant and animal tissues) and the challenges of substance-by-substance risk assessment and management urgently need/require the implementation of currently in use methodologies along with the design of new analytical tools (Pan et al., 2020; Koch et al., 2020). Among fluorinated pollutants, perfluorooctanoic acid (PFOA, $C_8HF_{15}O_2$) has been widely investigated and

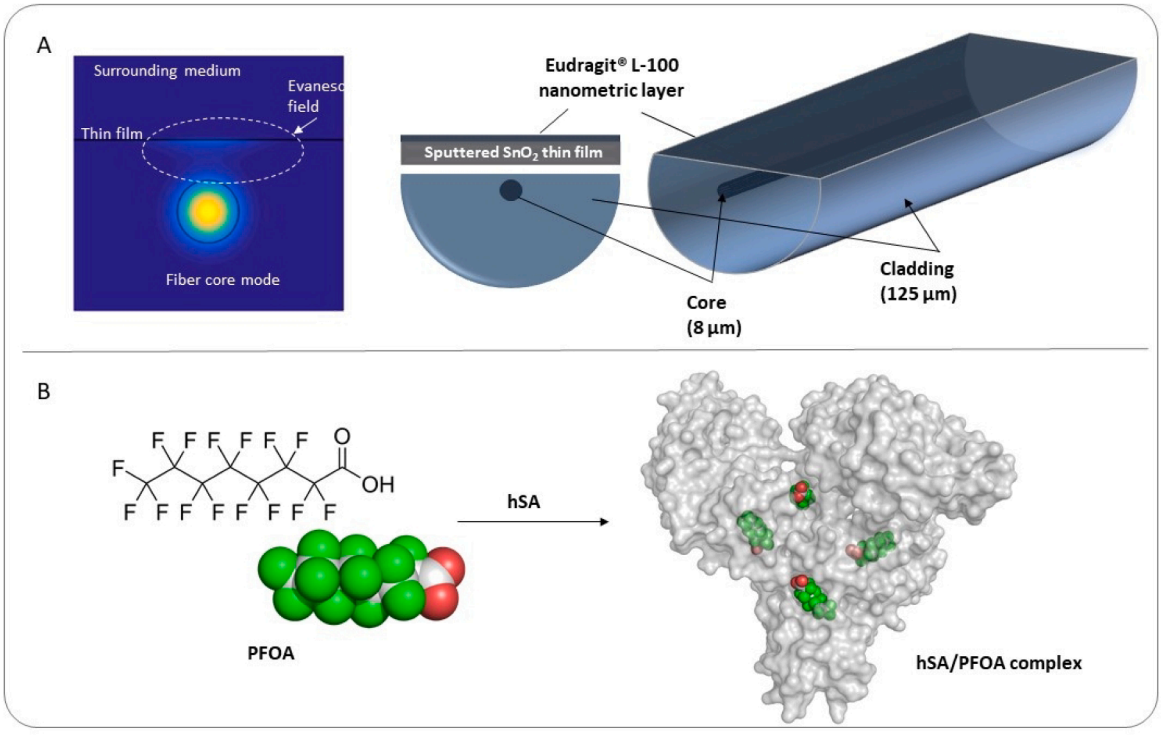

Fig. 1. Schematic representation of the nanocoated D-shaped fiber in use for the development of the sensing platform (A) and the chemical structure of the analyte, perfluorooctanoic acid (PFOA), which can form a 1:4 complex with human serum albumin (hSA/PFOA complex) (B).

serve as a model system for the development of PFAS sensing strategies (Cennamo et al., 2018; Cennamo et al., 2018; Fang et al., 2018). The interaction of PFOA with serum proteins, such as human serum albumin (hSA), has been extensively elucidated (Chi et al., 2018). Recently, Maso et al. reported the crystal structure of hSA in complex with four molecules of PFOA (Maso et al., 2021). They observed one high-affinity site (K_D = 0.35 μM) and three low-affinity sites (K_D = 27 μM). Structural analysis revealed the molecular basis of the intermolecular interactions among PFOA molecules and each binding site (Fig. 1B) (Maso et al., 2021). These findings might help designing high-specific medical treatment for the population that was overexposed to PFAS contamination as well as guiding the design of novel biosensing strategies to detect PFOA in drinking water samples using hSA as biological recognition element. Indeed, hSA presents numerous advantages compared to other biomolecules, such as antibodies: it is easily available, relatively stable at room temperature and has a cost-affordable pre-treatment.

Prior to apply delipidated hSA as a bioreceptor for PFAS monitoring, the complex stability was further investigated (Daems et al., 2021). The native mass spectrometry study proposed by Daems et al. (2021) confirmed the stability of delipidated hSA upon PFOA additions showing that delipidated hSA binds a larger number of PFOA molecules compared to the untreated protein. Delipidated hSA was finally tested at a confined-surface by an impedimetric sensor for monitoring of PFOA in water samples (Moro et al., 2020). In this sensing strategy, hSA was covalently immobilized on the surface of portable electrodes previously modified with a polymer rich in carboxylic moieties (Moro et al., 2020). The biolayer characterization showed that hSA was not denatured after immobilization. Moreover, the electrochemical impedance spectroscopy (EIS) data were supported by small-angle X-ray scattering confirming that hSA/PFOA complex has a more compact structure than the protein itself. These results have been the basis for the design of the optical sensing strategy, herein described. Indeed, hSA can be applied as bio-recognition layer also in optical platforms and the changes observed in hSA structure/conformation upon PFOA binding followed via EIS could be relevant for the development of a FO-based sensing strategy. In this context, we evaluated the applicability of delipidated hSA as a bioreceptor for PFOA detection in LMR-based sensing platforms. Delipidated hSA was covalently immobilized onto the SnO_{2-x} nanocoating of D-shaped FO. Different immobilization conditions were analysed, as described in the following paragraphs. After the functionalization of the FO surface, PFOA solutions at different concentrations were tested and preliminary conclusions drawn, revealing the ability of the sensor to detect very small molecules.

2. Materials and methods

2.1. Chemicals

The SnO_{2-x} target with 99.99% purity for the nanocoating deposition was purchased from ZhongNuo Advanced Material Technology Co. (Beijing, China). UV-polymerizing optical adhesive, NOA 68, Norland Products Inc. (East Windsor, NJ, US) was used. The recombinant human serum albumin (hSA, Albagen XL; UniProt ID: P02768) was purchased from Albumin Bioscience (Alabama, US). The charcoal was purchased by Caesar & Loretz GmbH. Methacrylic acid/methacrylate copolymer (Eudragit L100) was purchased from Evonik Degussa GmbH (Dusseldorf, Germany). 1-Ethyl-3-(3-(dimethylamino)-propyl) carbodiimide hydrochloride (EDC), and N-hydroxy succinimide (NHS) were purchased from Pierce (Illinois, US). Perfluorooctanoic acid (PFOA), NaH_2PO_4, Na_2HPO_4 and NaCl of analytical grade were purchased from Sigma-Aldrich (Milan, Italy). Phosphate buffer solution 0.1 M at pH 7.4 was prepared by mixing stock solutions of 0.1 M NaH_2PO_4 and 0.1 M Na_2HPO_4 and 0.1 M NaCl to obtain the corresponding saline buffer (PBS). All the buffers and solutions were of analytical grade and solutions were prepared using double distilled deionized water.

2.2. Bioreceptor preparation and purification

Delipidated plasma derived human serum albumin (hSA) was obtained by adsorption onto activated charcoal as previously described (Chi et al., 2018). Monomeric hSA was isolated from aggregates and disulfide-bridged dimers using a HiLoad 16/600 Superdex 200 prep grade size exclusion chromatography column (GE Healthcare) connected to an ÄKTA Pure 25 M system (GE Healthcare) and equilibrated with 50 mM PBS pH 7.4. Protein concentration was determined 280 nm using a mySPEC spectrophotometer (VWR). Purified defatted hSA protein was stored at −20 °C prior to use.

2.3. Fiber manufacturing and integration in the microfluidic system

As previously described (Zubiate et al., 2019), SnO_{2-x} nanocoated fibers were manufactured starting from the purchase of D-shaped fiber samples from Phoenix Photonics Ltd (Birchington, UK). The D-shaped fibers consisted of a standard single-mode fiber (i.e., Corning SMF-28e) with a side-polished region with a length of roughly 17 mm as sketched in Fig. 1A. Afterwards, the sensitive region, which is the polished surface of the fiber, was covered with the SnO_{2-x} nanocoating. The procedure for the deposition of the nanomaterial consisted of placing the fiber onto a suitable glassy substrate and then inserting it in a DC sputter machine (ND-SCS200, Nadetech Innovations; Navarra, Spain). Partial pressure of argon of 9×10^{-2} mbar and intensity of 90 mA were the parameters used for the deposition of SnO_{2-x} nanocoating. The size of the sputtering target was 57 mm in diameter and 3 mm in thickness. As already showed, these choices guarantee a thickness of the nanomaterial ranging from 150 nm to 180 nm (Zubiate et al., 2019), which is perfectly suitable for the excitation of first (with highest sensitivity) LMR in the infrared region (Nazri et al., 2021).

A custom-made experimental setup was built up in order to monitor the transmission spectrum of the fiber during the biosensing tests as showed in Fig. 2. It consisted of a broadband multi-LED light source (SLD-1310/1430/1550/1690; FiberLabs, Inc., Saitama, Japan) to guide the light through the fiber, of an optical spectrum analyzer (OSA, Anritsu MS9030A-MS9701B; Kanagawa, Japan) to monitor the LMR in a wide range from 1250 to 1700 nm, of a FO in-line polarizer and of a polarization controller, which permits to adjust the polarization state of light (TE or TM), placed between the optical source and the D-shaped fiber. After the deposition process, the fiber was placed inside a thermo-stabilized microfluidic system (Trono et al., 2011). The developed system permitted to control and manipulate small volumes of liquid samples in the order of μL, and to stabilize the temperature inside the flow channel with an error of ±0.05 °C. As shown in the enlargement of Fig. 2, the microfluidic system was made up of two equal-size pieces (74 mm long, 15 mm wide and 5 mm high each bar), which were assembled and sealed with Parafilm® sheet interposed between them in order to assure the water-proofing. The two bars consisted of PMMA (top) and of stainless steel (bottom). The flow channel was equally fabricated on both bars with a cross-sectional square size of 1 mm^2 and a length of 40 mm. Two stainless-steel tubes (1.2 mm outer diameter and 1 mm inner diameter) placed on the top bar acted as the inlet and outlet of the flow channel. In addition, a V-groove of 0.5 mm deep was engraved on both ends of the PMMA bar in order to house the D-shaped portion of the fiber, which was finally glued with its jacket to the V-groove edges using the UV-polymerizing optical adhesive. The bottom bar was thermally stabilized using two Peltier cells driven by a suitable controller (ILX Lightwave LDC-3722B TEC controller; ILX Lightwave Corporation, Bozeman, MT, US). A thermistor was laterally inserted into a hole in the PMMA bar to record the temperature during long-term experiments with the aid of a thermometric measuring unit (Lutron TM-917). Finally, the microfluidic system was connected to a peristaltic pump (GILSON Minipulse 3; Middleton, WI, US) by means of a premium medical grade plastic tubing, which made it possible to pump any solution into the flow channel at controlled rate. The flow rate changed according to the

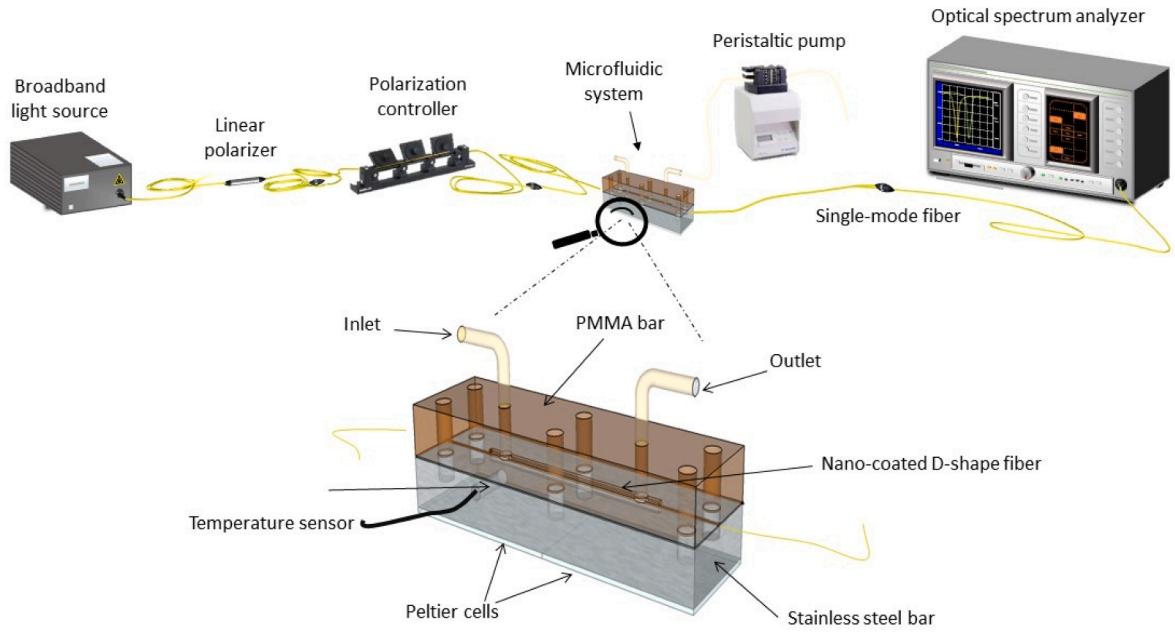

Fig. 2. Experimental setup for monitoring in real time the biological interaction of molecules through an SnO_{2-x} nanocoated D-shaped fiber. The enlargement details the developed microfluidic system and flow channel with the temperature-stabilization system.

biosensing protocol detailed in Section 2.5.

2.4. Fiber surface functionalization with hSA

The sensitive portion of the SnO_{2-x} nanocoated D-shaped fibers was functionalized by means of the deposition of Eudragit L100. The D-shaped part was immersed for 1 min in a solution of 0.04 % (w/v) Eudragit L100 in ethanol. Afterwards, the polymerization was completed after the total evaporation of the solvent (about 15 min). The polymeric film provides carboxylic moieties (–COOH) which enable the covalent immobilization of the hSA bioreceptor on the FO surface via 1-ethyl-3-(3-dimethylaminopropyl)carbodiimide hydrochloride/N-hydroxysuccinimide (EDC/NHS) coupling, as previously reported (Zubiate et al., 2019; Chiavaioli et al., 2017). At this point, the FO was positioned along the flow channel of the microfluidic system and glued with the UV-polymerizing optical adhesive. The temperature of the microfluidic system was set to the constant value of 15 °C. It should be noted that this value was different from those routinely used in the past literature ranging from 22 °C up to 30 °C (Zubiate et al., 2019; Chiavaioli et al., 2017). The temperature was set to 15 °C to preserve the conformation and biochemical activity of delipidated hSA avoiding altering the binding process in its kinetic and thermodynamic aspects (i.e. affinity constants, entropy/enthalpy-driven interactions). The carboxylic groups were activated with EDC/NHS (2 mM/5 mM, respectively) solution injected at 25 μL min^{-1} for 30 min. Then, a 1 mg mL^{-1} solution of hSA was injected at different flow rates for 30 min or 1 h (specifications in Section 3.1). This step was followed by a washing step in PBS running buffer at a flow rate of 250 μL min^{-1} for 10 min. All solutions mentioned below were freshly prepared in PBS pH 7.4.

2.5. Protocol for PFOA sensing

The assays were performed injecting increasing concentrations of PFOA, considering two ranges of concentrations: from 15.6 ng mL^{-1} to 625 ng mL^{-1} (first range) and from 0.156 ng mL^{-1} to 15.6 ng mL^{-1} (second range). In both cases, a flow rate of 25 μL min^{-1} for roughly 30 min was used. Washing steps were performed with PBS after each PFOA injection, at a flow rate of 250 μL min^{-1} for 10/20 min when the steady-state condition was reached.

2.6. Scanning electron microscopy imaging

The morphology of the FO after functionalization was characterized using a scanning electron microscope (SEM; Gaia 3 Tescan FIB-SEM; TESCAN ORSAY HOLDING, a.s., Brno – Kohoutovice, Czech Republic), with an in-lens detector at 3 kV and an aperture diameter of 30 μm. The SEM is equipped with the X-ray microanalysis system (EDAX; Octane Elect EDS system; AMETEK, US) that was used for analysing the elemental composition of the FO samples in both its longitudinal and transversal cross-section.

3. Results and discussion

3.1. FO Functionalization: optimization of the protocol

In the design of SnO_{2-x} nanocoated D-shaped FO biosensing platforms, the integration of the biological sensing layer with the FO surface represents a crucial step. Therefore, flow parameters (i.e., flow rate and duration), reagents concentrations as well as other working conditions (i.e. temperature of the microfluidic system) need to be optimized to assure a stable, reproducible, performing modification of the FO, and hence to prevent the bioreceptor alteration. The covalent immobilization of hSA biosensing layer onto the fiber was carried out via EDC/NHS chemistry using the carboxylic moieties of a polymeric layer (Eudragit L100) deposited around the fiber surface before. The successful deposition of the acrylic/methacrylic esters polymer with this protocol was previously verified and the estimated thickness is about 60 nm (Zubiate et al., 2019). For the design of the following steps, two sets of conditions (namely protocol A and B) were tested to identify the best flow rate and duration for hSA immobilization step. It is worth noting that short modification protocols (<2 h) can result in unstable modifications due to the low amount of biomolecules immobilized; while, long modification protocols (>2 h) might be difficult to reproduce due to the partial alteration of the protein bioreceptor (i.e. conformational changes, unfolding) (Borisov and Wolfbeis, 2008). These considerations are instrumental to govern the complexity of biosensor design where immobilization/collection rates, equilibration steps and flow rate values play a key-role not only in the bioreceptor immobilization step, but also in the target recognition process, as thoroughly described by the

computational mode approach of Squires et al. (Squires et al., 2008).

Here, two protocols named A and B differing mainly for the flow rate used in hSA immobilization step of 25 μL/min and 10 μL/min, respectively, were applied. The sensorgrams (signal change vs time), showed in Fig. 3A, allow a direct comparison of the results. Using protocol A, hSA immobilization experienced a steeper change in the LMR signal and reached the stabilization in less than 30 min. For protocol B, the immobilization step of hSA lasted 1 h with a slower stabilization trend. A reduced flow rate implies a slower immobilization process of the bioreceptor; however, this does not mean that the assay could not benefit from a slower bioreceptor immobilization. In fact, this phenomenon was already seen in past literature (Zubiate et al., 2019) and would seem to be the most true when small size molecules are considered.

Here, the best conditions were selected considering the response of the biosensors upon addition of increasing concentrations of PFOA in low ng mL^{-1} range. An addition of 15.6 ng mL^{-1} resulted in a LMR

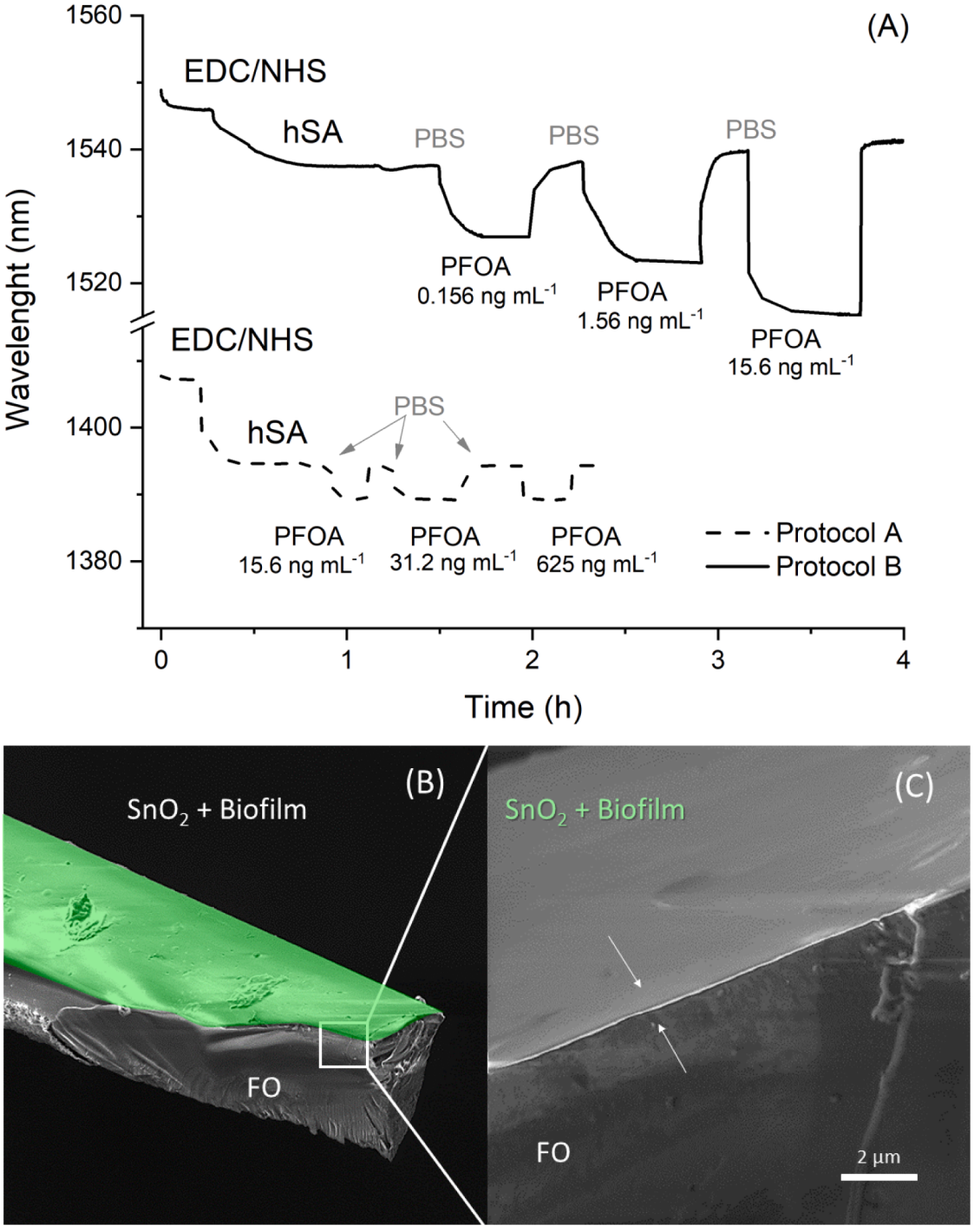

Fig. 3. (A) Comparison of the sensorgrams of the SnO_{2-x} nanocoated D-shaped fiber biosensors highlighting the modification steps using protocol A (dashed line) and B (continuous line): starting from the addition of EDC/NHS to the immobilization of delipidated albumin, the washing steps in PBS running buffer and the addition of the target, perfluorooctanoic acid (PFOA). SEM images of both the longitudinal (B) and cross-sectional (C) views of the functionalized silica fiber: the D-shaped region of the fiber with the modified surface (light green) and a zoom in the interface between the silica fiber (FO) and the SnO_{2-x} nanocoating modified with the biofilm. (For interpretation of the references to colour in this figure legend, the reader is referred to the web version of this article.)

residual shift (i.e., the shift of the baseline in PBS running buffer taken before and after the analyte injection) of 0.03 nm and of 3.7 nm with protocol A and B, respectively. Protocol A was found to lead to the formation of a non-suitable biological recognition layer: incubating PFOA spiked solutions with increasing concentrations (from 15.6 ng mL^{-1} to 31.2 and 625 ng mL^{-1}), no meaningful correlation with LMR residual shifts was observed in Fig. 3A. Even after incubation of high excess of PFOA (625 ng mL^{-1}) only a minimal LMR residual shift of 0.17 nm was recorded. The outcomes obtained after protocol A were ascribed to the different properties of the biological recognition layer. This do not exclude that tuning the target flow rate and increasing the collection time together with the system equilibration time would result in better performances (Chiavaioli et al., 2017). In fact, protocol B provided a stable modification, and even the incubation of a very low concentration of PFOA (0.156 ng mL^{-1}) resulted in a clear LMR shift, while the following additions of PFOA (1.56 and 15.6 ng mL^{-1}) exhibited increasing and larger shifts of the LMR wavelength.

To avoid a time-consuming optimization process for protocol A, protocol B was selected and considered suitable for the proposed application. Indeed, protocol B allows recording meaningful LMR residual shifts upon the incubation of increasing PFOA concentrations. Once identified a suitable set of conditions for the fiber functionalization, a section of the functionalized FO was analyzed by SEM imaging considering the flat surface of the D-shaped fiber portion. A layer brighter than the silica fiber was observed and was coloured in green for the sake of clarity given the label-free nature of the approach used (Fig. 3B). The layer comprises the biological (functionalization layer) and tin dioxide (LMR-exciting layer) nanocoatings. In its overall, the combined layers showed an average thickness of about (200 ± 15) nm as showed in Fig. 3C.

In the next steps, the biosensor capability to detect in real-time the PFOA/hSA binding interactions was screened.

3.2. PFOA determination: preliminary tests

Once the biological sensing layer preparation protocol was verified, increasing concentrations of PFOA spiked in PBS solutions were injected using the peristaltic pump, within the microfluidic system where the functionalized FO was previously located. For these preliminary experiments, PFOA concentrations of 0.156 ng mL^{-1} (PFOA1), 1.56 ng mL^{-1} (PFOA2) and 15.6 ng mL^{-1} (PFOA3) were tested aiming at demonstrating the range of applicability of the biosensor and its effectiveness in real scenario. An example of PFOA real-time monitoring is reported in Fig. 4A that represents the part of the entire sensorgram showed in Fig. 3A (protocol B) related to the interaction of PFOA with hSA-modified sensing layer: it starts with PBS addition, then the blank measurement (i.e., zero analyte concentration), followed by increasing PFOA concentrations.

Each sample incubation was followed by an intermediate washing step with PBS as well, to prevent nonspecific binding and analyte aggregation, and also to measure the real amount of attached biomolecules onto the fiber surface (Chiavaioli et al., 2017). The trend of LMR shift vs PFOA concentration is reported in Fig. 4B, while the experimental data were fitted using a Langmuir adsorption isotherm making use of Hill equation, which can model reversible association, such as complex formation, among a protein and a small size molecule ligand giving information about the degree of interaction (Gesztelyi et al., 2012). It is worth noticing that Hill equation was previously applied in LMR-based biosensors (Zubiate et al., 2019) and other types of biosensors (Cennamo et al., 2018). The sigmoidal fitting in Fig. 4B showed a correlation coefficient R^2 of 0.9989 with a maximum standard deviation of about 0.06 nm (hence the standard deviation bars are not visible in the plot). The values of the standard deviation were obtained by considering 20 consecutive acquisitions for each experimental point under the same working conditions at flow stopped and after reaching the equilibrium. By using the approach described in (Chiavaioli et al., 2017) where the maximum standard deviation of the experimental points can be considered (conservative approach), an idea of the limit of detection (LOD) is provided by a concentration value below 0.1 ng mL^{-1}, so very close to the PFOA concentration limits required by the current regulation. These preliminary results suggest the possibility to detect PFOA concentrations even below 0.156 ng mL^{-1}.

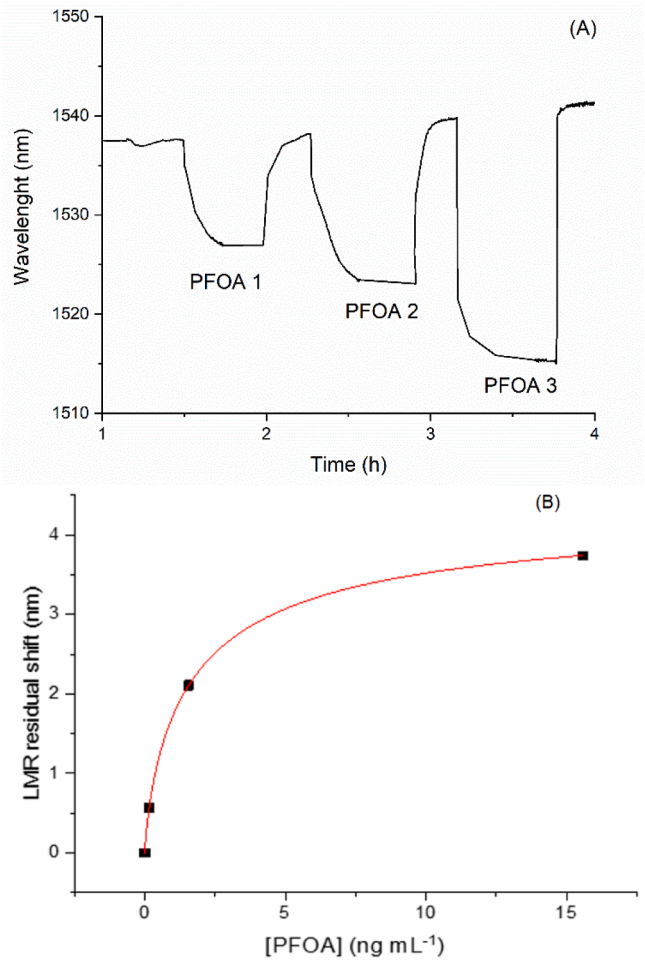

Fig. 4. (A) Example of part of the sensorgram of the SnO2-x nanocoated LMR fiber biosensor as a function of increasing concentrations of PFOA: 0.156 ng mL^{-1} (PFOA 1), 1.56 ng mL^{-1} (PFOA 2), 15.6 ng mL^{-1} (PFOA 3) (B) Calibration curve fitted with a Langmuir adsorption isotherm (sigmoidal curve) based on Hill equation.

After PFOA additions, the presence of fluorine caused by the PFOA binding to hSA (see PFOA structure in Fig. 1B) was further confirmed via SEM-EDS–based analysis, considering the central flat surface of the SnO_{2-x} nanocoated D-shaped FO, as showed in the inset of Fig. 5. Fluorine is found to be 3.72 wt%, as reported in Table 1, while the functionalization layer (biofilm plus tin dioxide layer) is responsible for the presence of both carbon (14.31 wt%) and tin dioxide (30 wt%). These data clearly confirmed that, after the incubation step, PFOA was confined at the FO surface even after the washing steps in running buffer. Therefore, it is possible to conclude that the analyte is not non-specifically bound to the protein layer of the FO surface, but it is able to give high-affinity non-covalent interactions with the biofilm that allow a stable confinement of the PFOA itself onto the FO surface. This was further confirmed with the absence of fluorine in SEM-EDS–based analysis from a pristine SnO_{2-x} nanocoated D-shaped FO sample (see Table 1, row named "No PFOA"). These preliminary findings suggest the interest of improving this sensing strategy and support the current dataset with negative control experiments and a complete interference study.

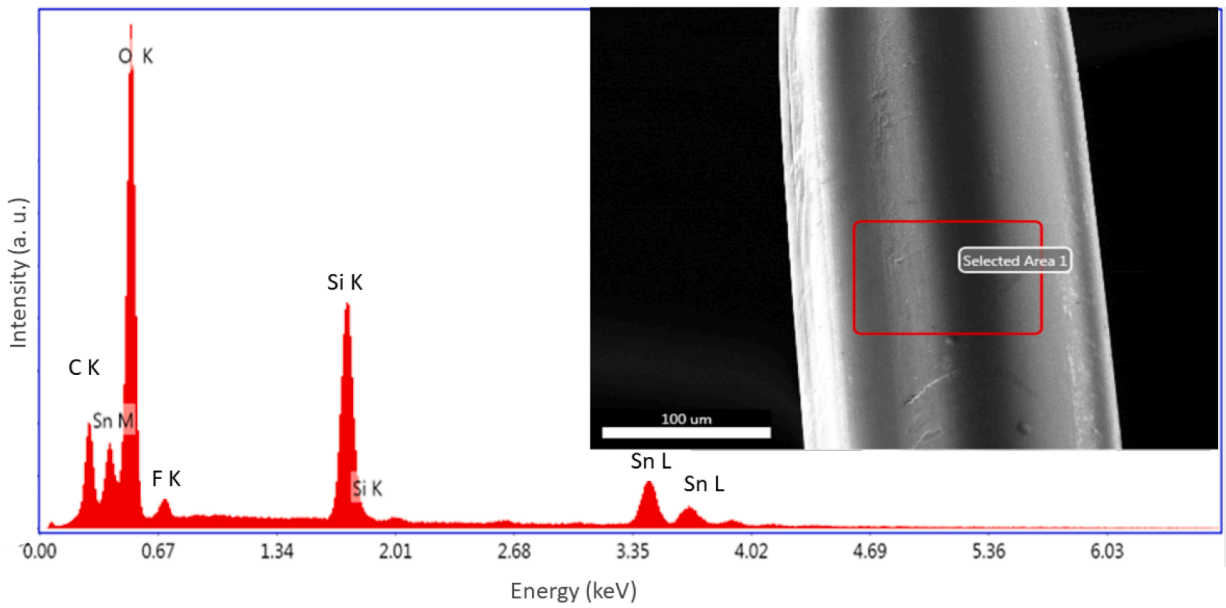

Fig. 5. EDS spectrum of an area of the flat surface of SnO_{2-x} nanocoated D-shaped FO after incubation of PFOA synthetic solutions; the area selected is highlighted in the SEM image reported in the inset (red box). (For interpretation of the references to colour in this figure legend, the reader is referred to the web version of this article.)

Table 1
Chemical composition of the SnO_{2-x} nanocoated D-shaped FO after PFOA tests and comparison with a pristine FO sample (no PFOA tests).

	Element	Carbon (K)	Oxygen (K)	Silicon (K)	Fluorine (K)	Tin (L)
No PFOA	wt %	17.44	32.79	21.87	0.00	27.90
PFOA	wt %	14.31	32.74	19.23	3.72	30.00

4. Conclusions

The applicability of delipidate hSA in PFOA sensing based on FO via LMR was investigated in this study. We showed the importance of designing a suitable functionalization protocol, testing at least two different sets of immobilization conditions for the deposition of the biological recognition layer. In optimized conditions, the biosensor response upon incubation of PFOA synthetic solutions with increasing concentrations showed a response that follows the typical Langmuir adsorption isotherm. The analysis of the chemical composition of the FO samples before and after the analysis was used to indirectly confirm the confinement of PFOA at the albumin functionalized fiber surface. Therefore, SEM-EDS–based analysis can be applied as a control technique once the sensor tests are completed.

This study suggests: the interest of performing further optimization of the LMR-based platform, the capability to determine PFOA in the low ng mL^{-1} range as required by the regulation limits for PFAS in waters and the compatibility of hSA/PFOA system with optical sensing, as the impedimetric approach (Moro et al., 2020). Furthermore, delipidated hSA can be engineered by selecting just the domains that showed the highest affinity for PFOA based on the crystallographic studies or modifying the protein structure to increase the bioreceptor affinity. Implementing the biological layer affinity for the target or amplifying its conformation changes in presence of these small-size molecules can be instrumental also in determining the sensor selectivity which plays a fundamental role considering the rapid evolution of this class of pollutants.

LMR-based sensing strategies can be further applied to other compounds of PFAS family by using different protein biological layers or engineered albumins (different domains or modification can lead to different selectivity in the final bioreceptor). These latter present all the advantages of highly stable, reproducible, and cost-affordable bioreceptors. We believe that this preliminary but disruptive study highlights how LMR-based sensing technology can rapidly evolve fulfilling the markets needs even in terms of monitoring small-size molecules, thus paving the way for a remarkable and almost-unique approach able to sense any kind of biological target (small, medium and large size molecules) with high-performance outcomes.

CRediT authorship contribution statement

Giulia Moro: Conceptualization, Methodology, Investigation, Writing - original draft. **Francesco Chiavaioli:** Conceptualization, Methodology, Investigation, Data curation, Writing - review & editing. **Stefano Liberi:** Methodology. **Pablo Zubiate:** Methodology. **Ignacio Del Villar:** Writing - review & editing. **Alessandro Angelini:** Methodology, Supervision. **Karolien De Wael:** Supervision. **Francesco Baldini:** Writing - review & editing, Supervision. **Ligia Maria Moretto:** Supervision. **Ambra Giannetti:** Conceptualization, Methodology, Writing - review & editing.

Declaration of Competing Interest

The authors declare that they have no known competing financial interests or personal relationships that could have appeared to influence the work reported in this paper.

Acknowledgments

This work was partially supported by the National Research Council of Italy (CNR) for the Short Term Mobility programs 2017 and 2019. We gratefully acknowledge Dr. Maria Cristina Salvatici (CNR-ICCOM) for the SEM-EDS measurements and Mr. Andrea Donati (CNR-IFAC) to the technical support for the realization of the microfluidic system used in

this work.

References

Abunada, Z., Alazaiza, M.Y.D., Bashir, M.J.K., 2020. An overview of per- and polyfluoroalkyl substances (PFAS) in the environment: source, fate, risk and regulations. Water 12. https://doi.org/10.3390/w12123590.

Bertanza, G., Capoferri, G.U., Carmagnani, M., Icarelli, F., Sorlini, S., Pedrazzani, R., 2020. Long-term investigation on the removal of perfluoroalkyl substances in a full-scale drinking water treatment plant in the Veneto Region, Italy. Sci. Total Environ. 734, 139154 https://doi.org/10.1016/j.scitotenv.2020.139154.

Borisov, S.M., Wolfbeis, O.S., 2008. Optical biosensors. Chem. Rev. 108 (2), 423–461. https://doi.org/10.1021/cr068105t.

Cardona-Maya, Y., Socorro, A.B., Del Villar, I., Cruz, J.L., Corres, J.M., Botero-Cadavid, J. F., 2018. Label-free wavelength and phase detection based SMS fiber immunosensors optimized with cladding etching. Sens. Actuat., B Chem. 265, 10–19. https://doi.org/10.1016/j.snb.2018.03.002.

Cennamo, N., Zeni, L., Tortora, P., Regonesi, M.E., Giusti, A., Staiano, M., D'Auria, S., Varriale, A., 2018. A high sensitivity biosensor to detect the presence of perfluorinated compounds in environment. Talanta 178, 955–961. https://doi.org/10.1016/j.talanta.2017.10.034.

Cennamo, N., D'Agostino, G., Sequeira, F., Mattiello, F., Porto, G., Biasiolo, A., Nogueira, R., Bilro, L., Zeni, L., 2018. A simple and low-cost optical fiber intensity-based configuration for perfluorinated compounds in water solution. Sensors (Basel) 18, 3009. https://doi.org/10.3390/s18093009.

Chi, Q., Li, Z., Huang, J., Ma, J., Wang, X., 2018. Interactions of perfluorooctanoic acid and perfluorooctanesulfonic acid with serum albumins by native mass spectrometry, fluorescence and molecular docking. Chemosphere 198, 442–449. https://doi.org/10.1016/j.chemosphere.2018.01.152.

Chiavaioli, F., 2020. Recent development of resonance-based optical sensors and biosensors. Optics 1. https://doi.org/10.3390/opt1030019.

Chiavaioli, F., Gouveia, C.A.J., Jorge, P.A.S., Baldini, F., 2017. Towards a uniform metrological assessment of grating-based optical fiber sensors: from refractometers to biosensors. Biosensors 7. https://doi.org/10.3390/bios7020023.

Chiavaioli, F., Janner, D., 2021. Fiber optics sensing with lossy mode resonances: applications and perspectives. J. Light. Technol. 8724 https://doi.org/10.1109/JLT.2021.3052137.

Chiavaioli, F., Zubiate, P., Del Villar, I., Zamarreño, C.R., Giannetti, A., Tombelli, S., Trono, C., Arregui, F.J., Matias, I.R., Baldini, F., 2018. Femtomolar detection by nanocoated fiber label-free biosensors. ACS Sensors 3 (5), 936–943. https://doi.org/10.1021/acssensors.7b00918.

Daems, E., Moro, G., Berghmans, H., Moretto, L.M., Dewilde, S., Angelini, A., Sobott, F., De Wael, K., 2021. Native mass spectrometry for the design and selection of protein bioreceptors for perfluorinated compounds. Analyst 146 (6), 2065–2073. https://doi.org/10.1039/D0AN02005B.

Dean, W.S., Adejumo, H.A., Caiati, A., Garay, P.M., Harmata, A.S., Li, L., Rodriguez, E.E., Sundar, S., 2020. A framework for regulation of new and existing PFAS by EPA. J. Sci. Policy Gov. 16.

Del Villar, I., Hernaez, M., Zamarreño, C.R., Sánchez, P., Fernández-Valdivielso, C., Arregui, F.J., Matias, I.R., 2012. Design rules for lossy mode resonance based sensors. Appl. Opt. 51, 4298–4307. https://doi.org/10.1364/AO.51.004298.

Esposito, F., Sansone, L., Srivastava, A., Baldini, F., Campopiano, S., Chiavaioli, F., Giordano, M., Giannetti, A., Iadicicco, A., 2021. Long period grating in double cladding fiber coated with graphene oxide as high-performance optical platform for biosensing. Biosens. Bioelectron. 172, 112747 https://doi.org/10.1016/j.bios.2020.112747.

Fang, C., Zhang, X., Dong, Z., Wang, L., Megharaj, M., Naidu, R., 2018. Smartphone app-based/portable sensor for the detection of fluoro-surfactant PFOA. Chemosphere 191, 381–388. https://doi.org/10.1016/j.chemosphere.2017.10.057.

Fiedler, H., Kennedy, T., Henry, B.J., 2020. A critical review of a recommended analytical and classification approach for organic fluorinated compounds with an emphasis on per- and polyfluoroalkyl substances. Integr. Environ. Assess. Manag. https://doi.org/10.1002/ieam.4352.

Gesztelyi, R., Zsuga, J., Kemeny-Beke, A., Varga, B., Juhasz, B., Tosaki, A., 2012. The Hill equation and the origin of quantitative pharmacology. Arch. Hist. Exact Sci. 66 (4), 427–438. https://doi.org/10.1007/s00407-012-0098-5.

Goodrow, S.M., Ruppel, B., Lippincott, R.L., Post, G.B., Procopio, N.A., 2020. Investigation of levels of perfluoroalkyl substances in surface water, sediment and fish tissue in New Jersey, USA. Sci. Total Environ. 729, 138839 https://doi.org/10.1016/j.scitotenv.2020.138839.

Homola, J., 2003. Present and future of surface plasmon resonance biosensors. Anal. Bioanal. Chem. 377 (3), 528–539. https://doi.org/10.1007/s00216-003-2101-0.

Jiao, L., Zhong, N., Zhao, X., Ma, S., Fu, X., Dong, D., 2020. Recent advances in fiber-optic evanescent wave sensors for monitoring organic and inorganic pollutants in water. TrAC, Trends Anal. Chem. 127, 115892 https://doi.org/10.1016/j.trac.2020.115892.

Khansili, N., Rattu, G., Krishna, P.M., 2018. Label-free optical biosensors for food and biological sensor applications. Sens. Actuat., B. Chem. 265, 35–49. https://doi.org/10.1016/j.snb.2018.03.004.

Koch, A., Aro, R., Wang, T., Yeung, L.W.Y., 2020. Towards a comprehensive analytical workflow for the chemical characterisation of organofluorine in consumer products and environmental samples. TrAC - Trends Anal. Chem. 123 https://doi.org/10.1016/j.trac.2019.02.024.

Kosiel, K., Koba, M., Masiewicz, M., Śmietana, M., 2018. Tailoring properties of lossy-mode resonance optical fiber sensors with atomic layer deposition technique. Opt. Laser Technol. 102, 213–221. https://doi.org/10.1016/j.optlastec.2018.01.002.

Kwiatkowski, C.F., Andrews, D.Q., Birnbaum, L.S., Bruton, T.A., DeWitt, J.C., Knappe, D. R.U., Maffini, M.V., Miller, M.F., Pelch, K.E., Reade, A., Soehl, A., Trier, X., Venier, M., Wagner, C.C., Wang, Z., Blum, A., 2020. Scientific basis for managing PFAS as a chemical class. Environ. Sci. Technol. Lett. 7 (8), 532–543. https://doi.org/10.1021/acs.estlett.0c00255.

Li, Z., Yang, X., Zhu, H., Chiavaioli, F., 2021. Sensing performance of fiber-optic combs tuned by nanometric films: new insights and limits. IEEE Sens. J. 1–12. https://doi.org/10.1109/JSEN.2021.3068445.

Maso, L., Trande, M., Liberi, S., Moro, G., Daems, E., Linciano, S., Sobott, F., Covaceuszach, S., Cassetta, A., Fasolato, S., Moretto, L.M., De Wael, K., Cendron, L., Angelini, A., 2021. Unveiling the binding mode of perfluorooctanoic acid to human serum albumin. Protein Sci. https://doi.org/10.1002/pro.4036.

Meyer, A.M., Klein, C., Fünfrocken, E., Kautenburger, R., Beck, H.P., 2019. Real-time monitoring of water quality to identify pollution pathways in small and middle scale rivers. Sci. Total Environ. 651, 2323–2333. https://doi.org/10.1016/j.scitotenv.2018.10.069.

Moro, G., Bottari, F., Liberi, S., Covaceuszach, S., Cassetta, A., Angelini, A., De Wael, K., Maria, L., 2020. Covalent immobilization of delipidated human serum albumin on poly (pyrrole-2-carboxylic) acid film for the impedimetric detection of perfluorooctanoic acid. Bioelectrochemistry 134, 107540. https://doi.org/10.1016/j.bioelechem.2020.107540.

Nakayama, S.F., Yoshikane, M., Onoda, Y., Nishihama, Y., Iwai-Shimada, M., Takagi, M., Kobayashi, Y., Isobe, T., 2019. Worldwide trends in tracing poly- and perfluoroalkyl substances (PFAS) in the environment. TrAC - Trends Anal. Chem. 121 https://doi.org/10.1016/j.trac.2019.02.011.

Nazri, N.A.A., Azeman, N.H., Luo, Y., A Bakar, A.A., 2021. Carbon quantum dots for optical sensor applications: A review. Opt. Laser Technol. 139, 106928. https://doi.org/10.1016/j.optlastec.2021.106928.

Pan, Y., Wang, J., Yeung, L.W.Y., Wei, S., Dai, J., 2020. Analysis of emerging per- and polyfluoroalkyl substances: Progress and current issues. TrAC - Trends Anal. Chem. 124 https://doi.org/10.1016/j.trac.2019.04.013.

Peltomaa, R., Glahn-Martínez, B., Benito-Peña, E., Moreno-Bondi, M.C., 2018. Optical biosensors for label-free detection of small molecules. Sensors 18. https://doi.org/10.3390/s18124126.

Pissadakis, S., 2019. Lab-in-a-fiber sensors: A review. Microelectron. Eng. 217, 111105. https://doi.org/10.1016/j.mee.2019.111105.

Ricciardi, A., Crescitelli, A., Vaiano, P., Quero, G., Consales, M., Pisco, M., Esposito, E., Cusano, A., 2015. Lab-on-fiber technology: a new vision for chemical and biological sensing. Analyst 140, 8068–8079. https://doi.org/10.1039/C5AN01241D.

Schubert, S.M., Arendt, L.M., Zhou, W., Baig, S., Walter, S.R., Buchsbaum, R.J., Kuperwasser, C., Walt, D.R., 2015. Ultra-sensitive protein detection via Single Molecule Arrays towards early stage cancer monitoring. Sci. Rep. 5, 11034. https://doi.org/10.1038/srep11034.

Shukla, S.K., Kushwaha, C.S., Guner, T., Demir, M.M., 2019. Chemically modified optical fibers in advanced technology: An overview. Opt. Laser Technol. 115, 404–432. https://doi.org/10.1016/j.optlastec.2019.02.025.

Śmietana, M., Koba, M., Mikulic, P., Bock, W.J., 2016. Towards refractive index sensitivity of long-period gratings at level of tens of μm per refractive index unit: fiber cladding etching and nano-coating deposition. Opt. Express 24, 11897–11904. https://doi.org/10.1364/OE.24.011897.

Squires, T.M., Messinger, R.J., Manalis, S.R., 2008. Making it stick: convection, reaction and diffusion in surface-based biosensors. Nat. Biotechnol. 26, 417–426. https://doi.org/10.1038/nbt1388.

Trono, C., Baldini, F., Brenci, M., Chiavaioli, F., Mugnaini, M., 2011. Flow cell for strain- and temperature-compensated refractive index measurements by means of cascaded optical fibre long period and Bragg gratings. Meas. Sci. Technol. 22 https://doi.org/10.1088/0957-0233/22/7/075204.

Vierke, L., Staude, C., Biegel-Engler, A., Drost, W., Schulte, C., 2012. Perfluorooctanoic acid (PFOA) — main concerns and regulatory developments in Europe from an environmental point of view. Environ. Sci. Eur. 24, 16. https://doi.org/10.1186/2190-4715-24-16.

Wang, Z., DeWitt, J., Higgins, C.P., Cousins, I.T., 2018. Correction to "A never-ending story of per- and polyfluoroalkyl substances (PFASs)?". Environ. Sci. Technol. 52, 3325. https://doi.org/10.1021/acs.est.8b00599.

Wang, X.-D., Wolfbeis, O.S., 2020. Fiber-optic chemical sensors and biosensors (2015–2019). Anal. Chem. 92 (1), 397–430. https://doi.org/10.1021/acs.analchem.9b04708.

Yaroshenko, I., Kirsanov, D., Marjanovic, M., Lieberzeit, P.A., Korostynska, O., Mason, A., Frau, I., Legin, A., 2020. Real-time water quality monitoring with chemical sensors. Sensor 20, 3432.

Zhang, Y.-N., Sun, Y., Cai, L., Gao, Y., Cai, Y., 2020. Optical fiber sensors for measurement of heavy metal ion concentration: A review. Measurement 158, 107742. https://doi.org/10.1016/j.measurement.2020.107742.

Zhao, Y., Hu, X.-G., Hu, S., Peng, Y., 2020. Applications of fiber-optic biochemical sensor in microfluidic chips: A review. Biosens. Bioelectron. 166, 112447. https://doi.org/10.1016/j.bios.2020.112447.

Zubiate, P., Urrutia, A., Zamarreño, C.R., Egea-Urra, J., Fernández-Irigoyen, J., Giannetti, A., Baldini, F., Díaz, S., Matias, I.R., Arregui, F.J., Santamaría, E., Chiavaioli, F., Del Villar, I., 2019. Fiber-based early diagnosis of venous thromboembolic disease by label-free D-dimer detection. Biosens. Bioelectron. X. 2, 100026 https://doi.org/10.1016/j.biosx.2019.100026.